



The relationships between urban landscape patterns and fine particulate pollution in China: A multiscale investigation using a geographically weighted regression model

Mengzhao Tu ^{a, b}, Zhifeng Liu ^{a, b}, Chunyang He ^{a, b, *}, Zihang Fang ^{a, b}, Wenlu Lu ^{a, b}

^a Center for Human-Environment System Sustainability (CHESS), State Key Laboratory of Earth Surface Processes and Resource Ecology (ESPRE), Beijing Normal University, Beijing, 100875, China

^b School of Natural Resources, Faculty of Geographical Science, Beijing Normal University, Beijing, 100875, China

ARTICLE INFO

Article history:

Received 9 April 2019

Received in revised form

19 July 2019

Accepted 21 July 2019

Available online 22 July 2019

Handling Editor: Giorgio Besagni

Keywords:

Urbanization

Urban landscape patterns

PM_{2.5} pollution

Geographically weighted regression

Urban sustainability

ABSTRACT

Providing accurate assessments of the relationships between urban landscape patterns and PM_{2.5} pollution is essential for improving urban sustainability in China. Accordingly, this paper uses a geographically weighted regression model to reveal the relationships between urban landscape patterns and PM_{2.5} pollution at different scales in China. First, we identified the level of PM_{2.5} pollution in China and quantified the urban landscape patterns based on the landscape metrics in 2015. Then, we analyzed the relationships between urban landscape patterns and PM_{2.5} pollution using geographically weighted regression with the county as the basic analytical unit. Finally, the spatial characteristics of the relationships between urban landscape patterns and PM_{2.5} pollution were analyzed at the national, regional and provincial scales. We found that the PM_{2.5} pollution in China was closely related to urban landscape patterns, with obvious spatial heterogeneity. The total area with a significant correlation between the urban landscape patterns (which were measured using the percentage of urban landscape, edge density, and patch density) and PM_{2.5} pollution ranged from 2.07×10^6 km² to 2.26×10^6 km², accounting for 42.55%–46.59% of the total PM_{2.5}-polluted area in China. The high correlations were concentrated mainly in five provinces, namely, Xinjiang, Shaanxi, Fujian, Chongqing and Guangdong. We also found that the relationships between urban landscape patterns and PM_{2.5} pollution were stronger in urban agglomerations. The total area with a significant correlation between the urban landscape patterns and PM_{2.5} pollution was 9.20×10^5 km², occupying 65.55% of the entire urban agglomeration area; this percentage was nearly 14% higher than the national average level. The strongest relationship was observed in the Northern Tianshan Mountains urban agglomeration. Contrasting with previous studies, our study fully considered the spatial autocorrelation and spatial differences between variables by using geographically weighted regression and clarified the spatial heterogeneity of the relationships between urban landscape patterns and PM_{2.5} pollution in China. Our findings imply that special attention must be paid to the urban landscape patterns in urban agglomerations during future urban development in China. Furthermore, effective regulations must be implemented to reduce the impacts of urban landscape patterns on PM_{2.5} pollution by controlling urban expansion and optimizing the spatial patterns of urban landscapes.

© 2019 Elsevier Ltd. All rights reserved.

1. Introduction

PM_{2.5} pollution refers to the presence of fine particulate matter in the atmosphere at a concentration and interval that causes it to interfere with the environment or the comfort, health and welfare of human beings (ISO, 1994; WHO, 2005). Urban landscape patterns (ULPs) refer to the composition and spatial configuration of urban landscape (i.e., the region dominated by non-vegetated, human-

* Corresponding author. State Key Laboratory of Earth Surface Processes and Resource Ecology, Beijing Normal University, 19 Xijiekouwai Street, Beijing, 100875, China.

E-mail addresses: tumengzhao@mail.bnu.edu.cn (M. Tu), zhifeng.liu@bnu.edu.cn (Z. Liu), hcy@bnu.edu.cn (C. He), zihangfang@mail.bnu.edu.cn (Z. Fang), Wenlu.Lu@mail.bnu.edu.cn (W. Lu).

constructed elements, such as roads, buildings, runways, and industrial facilities) (Forman, 2014; Liu et al., 2014). The ULPs affect PM_{2.5} pollution in two ways: first, ULPs alter anthropogenic PM_{2.5} emissions by changing resident travel modes and energy utilization behaviors as well as the industrial layout (Larkin et al., 2016). Second, ULPs alter PM_{2.5} pollution by influencing the regional climate and changing the diffusion conditions of atmospheric pollutants (Huang et al., 2014; Battaglia et al., 2017). From 1992 to 2015, the extent of urban land in China expanded from 12,000 km² to 73,000 km², representing a growth of 5 times (Xu et al., 2016b). Rapidly changing ULPs have led to the aggravation of PM_{2.5} pollution, which seriously threatens the health of residents and the sustainable development throughout China (Borrego et al., 2006; Xu et al., 2016a). Therefore, an accurate and effective assessment of the relationships between ULPs and PM_{2.5} pollution is of great significance for improving the urban environment, enhancing residential health conditions and achieving sustainable urban development in China (Han et al., 2014, 2015).

Many previous studies used the statistical ordinary least squares (OLS) model to reveal the relationships between ULPs and PM_{2.5} pollution in China. For example, Jiang et al. (2017) used the structural equation model to investigate the relationship between urban built-up areas and PM_{2.5} pollution in China, while Han et al. (2014) used correlation analysis to quantify the impacts of urban built-up areas on PM_{2.5} pollution in China. Lu et al. (2018) analyzed the relationship between the urban construction land area and PM_{2.5} pollution in the Yangtze River Delta (YRD) region using correlation analysis and multiple stepwise regression analysis. Similarly, Wu et al. (2015) employed multiple stepwise regression, correlation analysis and leave-one-out cross-validation to investigate the impact of the proportion of urban construction land on PM_{2.5} pollution in Beijing. However, few studies have accurately determined the relationships between ULPs and PM_{2.5} pollution, mainly because the OLS model is a global estimation method, which assumes that the relationships remain stable across space. Hence, this method reflects only global relationships, and thus, it lacks the ability to interpret spatial differences within those relationships (Du et al., 2018; Zhang and Gong, 2018). Nevertheless, the relationships between ULPs and PM_{2.5} pollution vary with geography and thus exhibit significant spatial heterogeneity and spatial autocorrelation (Yu et al., 2013). Therefore, it is difficult to effectively reveal the relationships between ULPs and PM_{2.5} pollution using the OLS model.

To more effectively quantify the relationships between ULPs and PM_{2.5} pollution in China, some researchers have used spatial econometric analysis to conduct relevant studies. For example, Yuan et al. (2018) selected 269 Chinese cities as sample cities and used the spatial lag model (SLM), the spatial error model (SEM) and the spatial Durbin model (SDM) to explore the impacts of ULPs on PM_{2.5} pollution. The spatial effects are considered in the SLM, SEM and SDM models, which can solve the spatial autocorrelation of PM_{2.5} concentration in nearby cities. However, these three models are essentially global regression models, and the constants and coefficients of the influencing factors in these models are the same in the different regions; thus, the spatial heterogeneity of the relationships between ULPs and PM_{2.5} pollution cannot be revealed (Yang et al., 2017). Therefore, it is necessary to use a new method to quantify the spatiotemporal patterns of the relationships between the ULPs and PM_{2.5} pollution throughout China.

The geographically weighted regression (GWR) model is a spatial analysis approach used to reveal the spatial relationships between variables by establishing local regression models for different regions within a certain spatial range (Fotheringham et al., 2002). In addition to fully considering the local effects of the relationships between variables in different regions, GWR detects the

spatial heterogeneity that can accurately and effectively reflect those relationships (Brunsdon et al., 1996, 1998; Su et al., 2012). In recent years, the GWR model has been widely employed to reveal the spatial patterns of the relationships between different variables. For example, Wang et al. (2018) used the GWR model to analyze the relationships among the spatiotemporal population distribution, land use and nighttime lights in China from 1990 to 2010, while Li et al. (2017) used the GWR model to evaluate the impacts of urbanization on the ULP in Beijing. Furthermore, Yu et al. (2013) detected the relationships between land use and water quality in Shenzhen based on GWR. Evidently, the GWR model provides an effective way to reveal the relationships between ULPs and PM_{2.5} pollution in China.

This study attempts to reveal the relationships between the ULPs and PM_{2.5} pollution throughout China. First, we analyzed the spatial patterns of PM_{2.5} pollution and quantified the ULP in 2015 at multiple scales. Then, we used the GWR model to analyze the relationships between ULPs and PM_{2.5} pollution at the national scale as well as at the regional and provincial scales. Finally, we discussed the advantages of the GWR model and the relationships between the ULP and PM_{2.5} pollution in China's major UAs. This study fully considers the spatial autocorrelation and spatial differences between variables using the GWR model, clarifies the spatial heterogeneity of the relationships between ULPs and PM_{2.5} pollution, and provides reliable support for urban landscape planning to improve the sustainability of cities in China.

2. Study area and data

2.1. Study area

We focused on the entire country of China and used 2359 counties as the basic analytical units (Fig. 1). We then analyzed the relationships between ULPs and PM_{2.5} pollution in China at the national, regional and provincial scales. According to the *Strategies and Policies for Regional Coordinated Development* issued by the Development Research Center of the State Council in 2005, China was divided into eight economic regions: Northeast China (NEC), Northern Coastal China (NCC), Eastern Coastal China (ECC), Southern Coastal China (SCC), Southwest China (SWC), Northwest China (NWC), the Middle Reaches of the Yellow River (MRYL), and the Middle Reaches of the Yangtze River (MRYTR). These economic regions were used as the statistical units at the regional scale, while the 34 provincial-level administrative regions in China were utilized as the statistical units at the provincial scale (Fig. 1).

2.2. Data

Urban land data for 2015 were obtained from the urban land information dataset in China established by He et al. (2014) and Xu et al. (2016b), and the data had a spatial resolution of 1 km. The data were produced using the support vector machine classification method by integrating the nighttime light data, land surface temperature data, and normalized difference vegetation index data. The overall accuracy of these data was 92.62%, the quantity disagreement was 1.49%, the allocation disagreement was 5.89%, and the Kappa coefficient was 0.60; thus, the data can accurately reflect the ULPs of China in 2015. Recently, urban land data have been widely used for analyzing the ULP and its impacts on environments in China. For instance, Liu et al. (2019) used the data to analyze the ULP and evaluate the impacts of ULP on the environmental sustainability of the agro-pastoral transitional zone of northern China.

The annual average PM_{2.5} concentration data for 2015 were obtained from "The global PM_{2.5} concentration dataset" released by



Fig. 1. Study area.

the Atmospheric Composition Analysis Group at NASA Langley Research Center for the removal of dust and sea salt. These data were produced based on the approach of the GEOS-Chem chemical transport model, with monitoring data acquired from NASA MODIS, MISR, and SeaWiFS. The $PM_{2.5}$ concentration in the dataset was in accordance with out-of-sample cross-validated $PM_{2.5}$ concentrations from monitors, with the R^2 reaching 0.81 (van Donkelaar et al., 2016).

The administrative boundaries of the entire country, provinces, and counties at a 1:1,000,000 scale were obtained from the National Geomatics Center of China.

3. Methods

3.1. Analyzing the distribution of $PM_{2.5}$ pollution

Referring to the study by He et al. (2016), we followed the air quality guideline (AQG) and the Interim Target-1 (IT-1) proposed by the World Health Organization, and we quantified the degree of $PM_{2.5}$ pollution for each county based on the annual average $PM_{2.5}$ concentration in 2015. The regions with $PM_{2.5}$ concentrations above the AQG ($10 \mu g/m^3$) were defined as polluted regions, and these areas included lightly polluted regions (AQG to IT-1, $10\text{--}35 \mu g/m^3$), moderately polluted regions (IT-1 to 2IT-1, $35\text{--}70 \mu g/m^3$) and heavily polluted regions ($>2IT-1$, $>70 \mu g/m^3$).

3.2. Quantifying the ULPs

Referring to the studies by Wu et al. (2011) and Liu et al. (2018a; 2018b), three landscape metrics were selected to quantify the ULP (Table 1). These landscape metrics included the percentage of urban land (PLAND), the patch density (PD) and the edge density (ED). Among them, the PLAND indicator measures the proportion of urban land in the landscape, the PD indicator quantifies the fragmentation of the urban landscape, and the ED indicator estimates the complexity of the urban landscape shape (Liu et al., 2018a). The three landscape metrics were selected because existing studies have revealed that these metrics can effectively represent ULPs and are highly correlated with $PM_{2.5}$ pollution. Generally, a larger PLAND value would result in more $PM_{2.5}$ pollutant emissions (Han et al., 2014). Higher PD and ED values represent more fragmented and complex-shaped ULPs, i.e., more dispersed infrastructures and services in residential, commercial and industrial areas, which subsequently increases the energy consumption from commuting, industrial processes and transportation and aggravates the emission of $PM_{2.5}$ pollutants (Larkin et al., 2016; Liu et al., 2019). In addition, the PLAND, PD and ED of urban land influence the regional climate and affect the diffusion of atmospheric pollutants (Irwin and Bockstael, 2007; Huang et al., 2014; Battaglia et al., 2017).

With the support of Fragstats and ArcGIS, we first calculated these three urban landscape metrics using the county as the basic unit in 2015. Then, we calculated the mean values of the

Table 1
The landscape metrics used in this study.

Metric	Equation	Unit Range	Description
Percentage of Urban Land (PLAND)	$PLAND = P_i = \frac{\sum_{j=1}^n a_{ij}}{A} \times 100$	% $0 < PLAND \leq 100$	The proportion of urban land in the landscape, where a_{ij} is the area (m^2) of patch ij ; A is the total landscape area (m^2).
Patch Density (PD)	$PD = \frac{n_i}{A} \times 10^6$	1/ $0 < PD$ km ²	The number of urban land patches per square kilometer. Higher values indicate more fragmented urban land. n_i represents the number of patches in the landscape of patch type i ; A is the total landscape area (m^2).
Edge Density (ED)	$ED = \frac{\sum_{k=1}^m e_{ik}}{A} \times 10^4$	m/ $0 < ED$ ha	The total edge length of urban land per hectare. Higher values indicate a more complex urban land shape. e_{ik} is the total length (m) of edge patch type i and includes landscape boundary and background segments involving patch type i ; A represents the total landscape area (m^2).

abovementioned metrics for the whole country, the economic regions, and the provinces. Finally, we used these mean values to analyze the spatial patterns of the urban landscape at the national, regional and provincial scales.

3.3. Quantifying the relationships between ULPs and PM_{2.5} pollution

The OLS model, a global regression model that reflects stationary and homogeneous relationships across space, can be expressed as follows:

$$y = \beta_0 + \sum_{k=1}^n \beta_k x_k + \epsilon \tag{1}$$

where y and x_k are the dependent variable and the k th independent variable, respectively, β_0 and β_k are the intercept and the local estimated coefficient, respectively, n represents the number of independent variables, and ϵ is the error term.

SLM is a spatial autoregressive model that describes the spatial correlation between dependent variables and mainly identifies whether variables have spillover effects in the study area. According to Anselin (1988), SLM can be expressed as follows:

$$y = \rho Wy + X\beta + \epsilon \tag{2}$$

where y is the dependent variable; X is an ($n \times k$) exogenous explanatory variable matrix; ρ is the auto-regressive parameter; W is an ($n \times k$) spatial weight matrix, usually the adjacency matrix; Wy is the spatial lag dependent variable of the spatial weight matrix W , which reflects the effect of the independent variable X on the dependent variable y ; and ϵ is the random error vector.

The spatial dependence of SEM exists in the random error term, which measures the influence of the error impact of the adjacent region on the observed value in the sample region. Anselin (1988) proposed the SEM as follows:

$$y = X\beta + \mu, \mu = \lambda W\mu + \epsilon \tag{3}$$

where y is the dependent variable; X is the ($n \times k$) matrix, which represents the explanatory variable; W is the spatial weight matrix; λ is the parameter of the spatial dependent error; β reflects the impacts of the independent variables on the dependent variable; μ is the ($n \times 1$) residual vector; and ϵ is the random error vector.

GWR is a local modeling tool optimized on the basis of the OLS model. The GWR model can be expressed as follows:

$$y_i = \beta_0(u_i, v_i) + \sum_{k=1}^n \beta_k(u_i, v_i)x_{ik} + \epsilon_i \tag{4}$$

where (u_i, v_i) represents the coordinates of sample point i ; y_i and x_{ik} are the dependent variable and the k th independent variable,

respectively, of the local regression model; $\beta_0(u_i, v_i)$ is the intercept; $\beta_k(u_i, v_i)$ is the local estimated coefficient; n is the number of independent variables; and ϵ_i is the error term. Data points that are closer to the location of the sample point are more spatially connected than those that are farther away, and thus, a distance decay function is needed to determine the weights of the data points within the spatial extent. Referring to the study by Yu et al. (2013), the bisquare weighting function was used in this study, and it can be expressed as follows:

$$W_{ik} = \left(1 - (d_{ik}/b)^2\right)^2 \tag{5}$$

where W_{ik} is the geographical weight of the k th data point with regard to sample point i , d_{ik} is the distance between sample point i and data point k , and b is the bandwidth, where a larger bandwidth corresponds to a wider extent of the local regression model. As d_{ik} becomes greater than b , the spatial weight turns to zero. Referring to the study by Fotheringham et al. (2002), the optimal bandwidth was selected according to the Akaike information criterion (AICc).

The output of the GWR model includes the adjusted R^2 , the t value, the local estimated coefficient and the local R^2 . Among them, the adjusted R^2 is a measure of the overall fitness of the model, ranging from the lowest fitness of 0 to the highest fitness of 1; a higher value indicates a better model fit. In addition, for each sample point, the local regression model contains a t value, a local estimated coefficient, and a local R^2 value. The t value is an index used to test the level of significance of the local estimated coefficient, while the local estimated coefficient is an index that characterizes the positive or negative relationships between the independent variables and the dependent variable; furthermore, the local R^2 is an index employed to measure the goodness-of-fit of the local regression model, where a higher local R^2 value reflects an independent variable with a stronger ability to interpret the dependent variable (Clement et al., 2009; Yu, 2006). In the model comparison section, we analyzed the abilities of the above four models to address the spatial autocorrelation of variables by calculating the global Moran's I of the residuals. Moran's I is an important indicator used to measure spatial correlation, and it tests whether adjacent regions in the whole study area are positively correlated, negatively correlated or mutually independent. The formula of Moran's I is as follows:

$$I = \frac{n \sum_{i=1}^n \sum_{j=1}^n W_{ij}(x_i - \bar{x})(x_j - \bar{x})}{\sum_{i=1}^n \sum_{j=1}^n W_{ij}(x_i - \bar{x})^2} = \frac{\sum_{i=1}^n \sum_{j \neq 1}^n W_{ij}(x_i - \bar{x})(x_j - \bar{x})}{S^2 \sum_{i=1}^n \sum_{j=1}^n W_{ij}} \tag{6}$$

where n is the total number of regions in the study area, W_{ij} is the spatial weight, x_i and x_j are the attributes of region i and region j , respectively, \bar{x} is the average value of all attributes, and S^2 is the variance of the attributes.

Based on the GWR model, we analyzed the relationships between the ULPs and PM_{2.5} pollution in China in 2015. To achieve this purpose, we quantified only the relationships between the ULP metrics and PM_{2.5} concentrations in the PM_{2.5} polluted regions, i.e., the regions with PM_{2.5} concentrations above the AQG (10 µg/m³), while the other regions were excluded from this analysis. First, we performed the GWR model using the county as the basic unit, with the annual average PM_{2.5} concentration in 2015 as the dependent variable and the PLAND, PD, and ED indicators as the independent variables. Specifically, we used the GWR model to quantify the relationships between PLAND and PM_{2.5} pollution, between PD and PM_{2.5} pollution, and between ED and PM_{2.5} pollution. Then, referring to the study by Tu (2011), we identified the counties where the PM_{2.5} pollution was significantly and positively correlated with the three urban landscape metrics according to the t value and the local estimated coefficient. In addition, we identified the counties where the local R² was greater than 0.5 (i.e., where the urban landscape metrics explained more than 50% of the variance in the PM_{2.5} pollution therein) as the area with the strong relationships between the urban landscape metrics and PM_{2.5} pollution. Finally, we quantified the total area of the identified counties and used the total area as an indicator to analyze the spatial relationships between the ULPs and PM_{2.5} pollution in 2015 at the national, regional, and provincial scales (Fig. 2).

4. Results

4.1. The distribution of PM_{2.5} pollution

In 2015, PM_{2.5} pollution was present in more than half of China's terrestrial area (Fig. 3, Table 2). Specifically, the total area of all

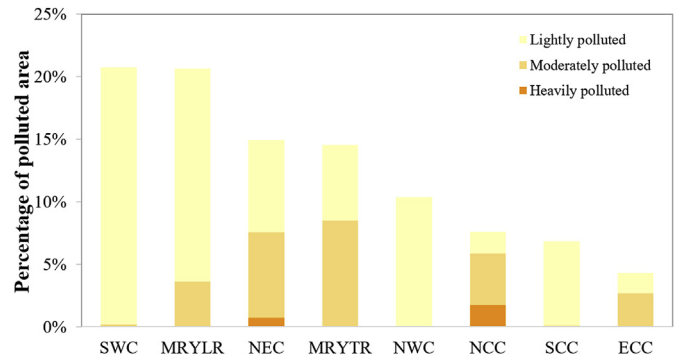


Fig. 3. PM_{2.5} pollution in China in 2015.

Note: The percentage of polluted area in each economic region relative to the polluted area in the whole country is shown in the figure.

PM_{2.5}-polluted regions was 4.86×10^6 km², accounting for 51.09% of China's entire land area. Among these areas, the areas of the lightly polluted regions, moderately polluted regions and heavily polluted regions were 3.71×10^6 km², 1.26×10^6 km² and 1.24×10^5 km², respectively, accounting for 36.53%, 13.27% and 1.30%, respectively, of China's total land area.

The PM_{2.5} pollution in China exhibited significant regional differences (Fig. 3, Table 2). Among the eight economic regions, the PM_{2.5}-polluted regions in SWC and MRYLR were relatively large, with areas of 1.01×10^6 km² and 1.00×10^6 km², respectively, which collectively occupied more than 20% of the total polluted area in China. The PM_{2.5}-polluted regions in NCC, SCC and ECC were relatively small, with areas of 3.70×10^5 km², 3.32×10^5 km² and

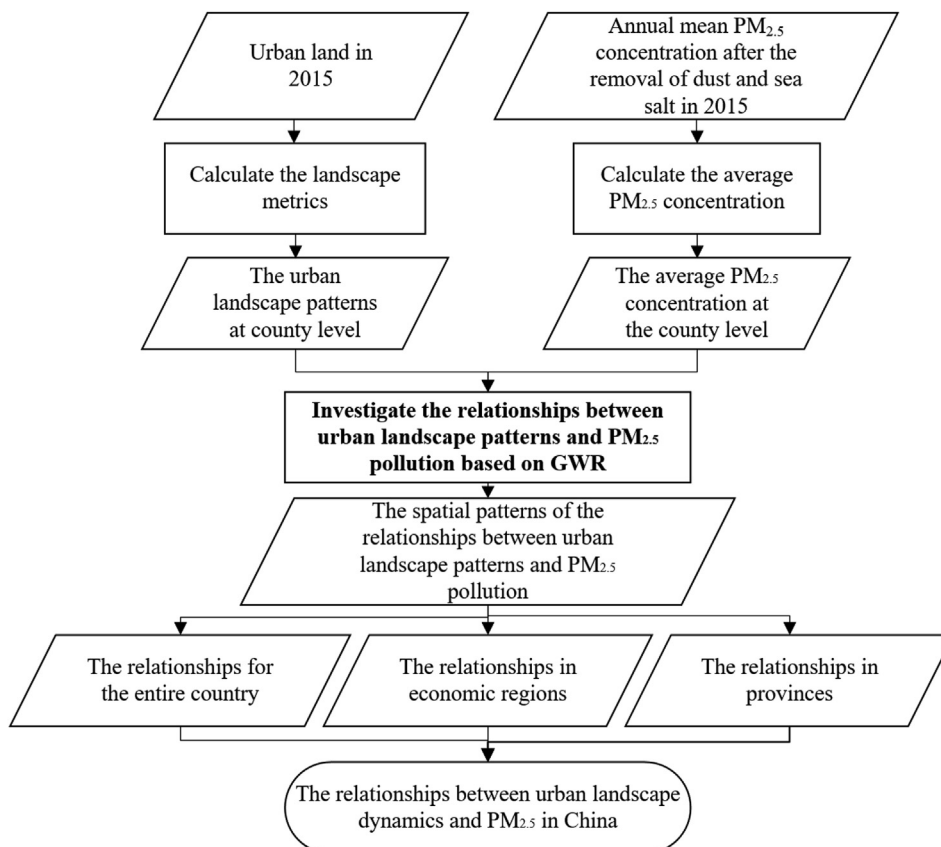


Fig. 2. Flow chart.

Table 2
The extents of polluted areas across each economic region in China and in the entire country.

Regions	Heavily polluted			Moderately polluted			Lightly polluted			Polluted area		
	Area (10 ⁴ km ²)	Per _N (%)	Per _E (%)	Area (10 ⁴ km ²)	Per _N (%)	Per _E (%)	Area (10 ⁴ km ²)	Per _N (%)	Per _E (%)	Area (10 ⁴ km ²)	Per _N (%)	Per _E (%)
NCC	8.47	0.89	22.92	20.12	2.12	54.45	8.36	0.88	22.62	36.95	3.89	100
ECC	0.27	0.03	1.30	12.74	1.34	60.91	7.91	0.83	37.79	20.92	2.20	100
MRYTR	0	/	/	41.25	4.34	58.48	29.28	3.08	41.52	70.53	7.42	100
NEC	3.60	0.38	4.57	33.16	3.49	42.01	35.70	3.76	45.23	72.46	7.62	91.81
SCC	0	/	/	0.39	0.04	1.01	32.85	3.46	85.10	33.24	3.50	86.11
SWC	0	/	/	0.87	0.09	0.64	99.90	10.51	73.26	100.77	10.60	73.90
MRYLR	0	/	/	17.54	1.85	10.48	82.77	8.71	49.44	100.31	10.55	59.92
NWC	0	/	/	0.00	0.00	0.00	50.38	5.30	12.57	50.38	5.30	12.57
The entire country	12.35	1.30	/	126.07	13.27	/	347.14	36.53	/	485.56	51.09	/

Note: Per_N: The ratio of the polluted area to the total land area of the entire country.
Per_E: The ratio of the polluted area to the total area of the corresponding economic region.

2.09 × 10⁵ km², respectively, all of which occupied less than 10% of the entire polluted area in China.

The areas with severe PM_{2.5} pollution were mainly concentrated in Northeast China, North China and East China (Fig. 3). The total areas of all heavily polluted and moderately polluted regions in NCC, ECC, MRYLR and NEC were 2.86 × 10⁵ km², 1.30 × 10⁵ km², 4.13 × 10⁵ km² and 8.17 × 10⁴ km², respectively, occupying 77.37%, 62.21%, 58.48% and 46.58%, respectively, of the total land area of the corresponding economic regions. Such proportions all exceeded the national average level (14.57%). Among these economic regions, the PM_{2.5} pollution was the most serious in NCC; the total areas of the heavily polluted regions and moderately polluted regions in NCC were 8.47 × 10⁴ km² and 2.01 × 10⁵ km², respectively, accounting for 22.92% and 54.45%, respectively, of the entire area of NCC.

4.2. The spatial patterns of the urban landscape

The ULP showed obvious spatial heterogeneity in China (Fig. 4, Table 3). In 2015, at the national level, the average PLAND was 2.28%, the average PD was 0.0013/km², and the average ED was 0.20 m/ha (Fig. 4). Among the eight economic regions, ECC had the largest proportion of urban land, the most fragmented urban landscape and the most complicated urban landscape shape; the PLAND, PD and ED in ECC were 6.09%, 0.0030/km² and 0.53 m/ha, respectively, which were 1.67 times, 1.31 times and 1.65 times higher than the corresponding national average levels, respectively. In contrast, NWC had the lowest proportion of urban land and the urban landscape with the simplest configuration; specifically, the PLAND, PD and ED in NWC were 0.47%, 0.0005/km² and 0.06 m/ha, respectively, which were equal to 20.61%, 38.46% and 30.00% of the corresponding national average levels, respectively.

4.3. The relationships between ULPs and PM_{2.5} pollution

The relationships between the ULPs and PM_{2.5} pollution in China also exhibited obvious spatial heterogeneity. The total area with a significant correlation between the PLAND and PM_{2.5} pollution was 2.21 × 10⁶ km², which occupied 45.43% of the entire PM_{2.5}-polluted area in China (Fig. 5a, Table 4). Among the eight economic regions, NEC had the largest area (5.13 × 10⁵ km², which accounted for 70.06% of the total PM_{2.5}-polluted area in NEC), with a significant correlation between the PLAND and PM_{2.5} pollution (Fig. 5b). At the provincial scale, all of the polluted regions in Beijing, Shanghai, and Hong Kong had significant correlations between the PLAND and PM_{2.5} pollution (Fig. 5c). The total area with a strong relationship between the PLAND and PM_{2.5} pollution was 9.50 × 10⁴ km², which occupied 1.96% of the entire PM_{2.5}-polluted area in China. Furthermore, the PLAND distributions in Fujian and

Guangdong provinces were more closely related to the PM_{2.5} pollution than were those in the other provinces; in these two provinces, the areas with strong relationships were 4.34 × 10⁴ km² and 3.81 × 10⁴ km², occupying 35.75% and 21.52%, respectively, of the total PM_{2.5}-polluted area in the corresponding provinces.

The total area with a significant relationship between the PD and PM_{2.5} pollution was 2.07 × 10⁶ km², occupying 42.55% of the entire PM_{2.5}-polluted area in China (Fig. 6a, Table 4). NEC exhibited the largest total area (5.00 × 10⁵ km², accounting for 69.04% of the entire PM_{2.5}-polluted area in NEC), with a significant correlation between these two variables (Fig. 6b). At the provincial scale, all of the polluted regions in Beijing and Shanghai had significant correlations between the PD and PM_{2.5} pollution (Fig. 6c). Furthermore, the total area with a strong relationship between the PD and PM_{2.5} pollution was 1.96 × 10⁵ km², which occupied 4.04% of the entire PM_{2.5}-polluted area. These regions were mainly concentrated over an area of 9.87 × 10⁴ km² in Xinjiang, occupying 49.74% of the entire PM_{2.5}-polluted area in Xinjiang.

The total area over which the ED displayed a significant correlation with the PM_{2.5} pollution was 2.26 × 10⁶ km², occupying 46.59% of the entire area of polluted regions in China (Fig. 7a, Table 4). At the regional scale, NEC had the largest area (5.00 × 10⁵ km², accounting for 69.04% of the entire PM_{2.5}-polluted area in NEC), characterized by a significant correlation between the ED and PM_{2.5} pollution (Fig. 7b). At the provincial scale, all of the polluted regions in Beijing, Shanghai, and Hong Kong had significant correlations between the ED and PM_{2.5} pollution (Fig. 7c). In addition, the total area characterized by a strong relationship between the ED and PM_{2.5} pollution (local R² above 0.5) was 1.89 × 10⁵ km², occupying 3.89% of the total PM_{2.5}-polluted area in China. These regions were concentrated primarily in three provinces, namely, Fujian, Chongqing and Guangdong, where the total areas with strong relationships were 4.98 × 10⁴ km², 2.60 × 10⁴ km² and 4.86 × 10⁴ km², respectively, occupying 40.98%, 31.59% and 27.45%, respectively, of the total PM_{2.5}-polluted areas in the corresponding provinces.

5. Discussion

5.1. The GWR model can accurately reveal the relationships between the ULPs and PM_{2.5} pollution in China

Referring to the study by Wang et al. (2018), we selected the adjusted R² and the AICc to compare the goodness-of-fit among the GWR, OLS, SLM and SEM models. The adjusted R², which ranges from 0 to 1, reflects the proportion of the total variation in the dependent variable that can be explained by the independent variable in the regression model; a higher adjusted R² value indicates a better fit. The AICc, another measure of the model's

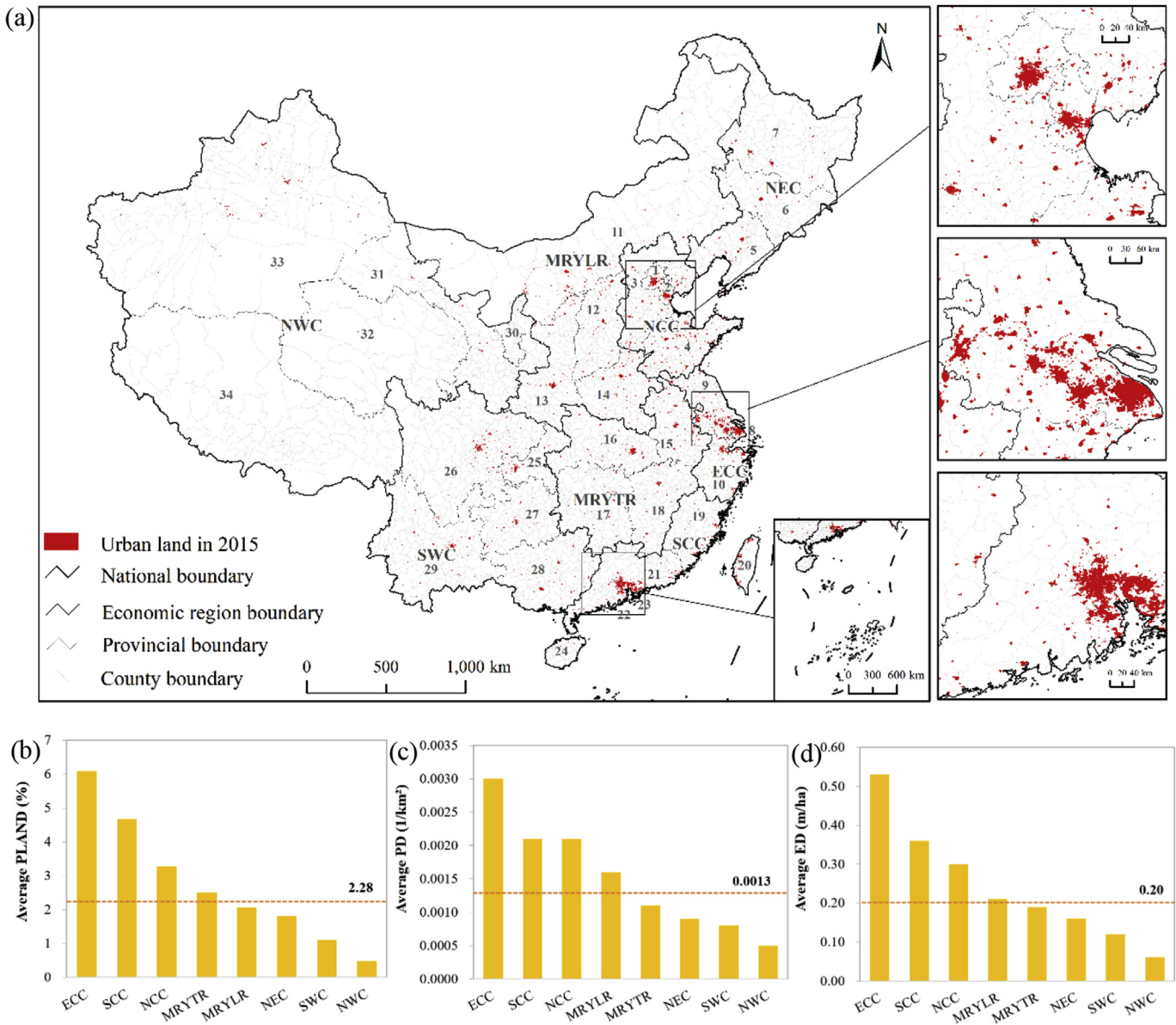


Fig. 4. The urban landscape patterns in China in 2015. (a) The spatial patterns of urban land. (b) The PLAND of urban land across each economic region. (c) The PD of urban land across each economic region. (d) The ED of urban land across each economic region. **Note:** The names of the economic regions are listed in Fig. 1.

goodness-of-fit, is based on the concept of entropy; a smaller AICc value indicates a better model performance (Clement et al., 2009; Yu, 2006). We found that the adjusted R² values of the GWR models

Table 3
The urban landscape patterns across the economic regions in 2015.

	Average PLAND (%)	Average PD (num/km ²)	Average ED (m/ha)
ECC	6.09	0.003	0.53
SCC	4.67	0.0021	0.36
NCC	3.27	0.0021	0.3
MRYLRL	2.51	0.0011	0.19
MRYLTR	2.06	0.0016	0.21
NEC	1.82	0.0009	0.16
SWC	1.1	0.0008	0.12
NWC	0.47	0.0005	0.06
The whole country	2.28	0.0013	0.2

were obviously higher than those of the other three models (Table 5). Moreover, the AICc values of the GWR models were lower than those of the other models. Therefore, among the four models, the GWR model was clearly best in terms of quantifying the relationships between the ULPs and PM_{2.5} pollution in China.

In addition, referring to the study by Tu (2011), we compared the abilities of the GWR and the OLS, SLM and SEM models to address the spatial autocorrelation of variables by calculating the global Moran's I of the residuals. We found that Moran's I for the OLS models ranged from 0.74 to 0.77, with a significant spatial autocorrelation (Table 5), whereas Moran's I for the SLM and SEM were 0.09 and 0.08, respectively, effectively removing the influence of spatial autocorrelation on the results. The range of Moran's I for the GWR models was 0.06–0.08, and the values in the GWR model were much smaller than those in the OLS models and slightly smaller than the values in SLM and SEM, demonstrating the spatial

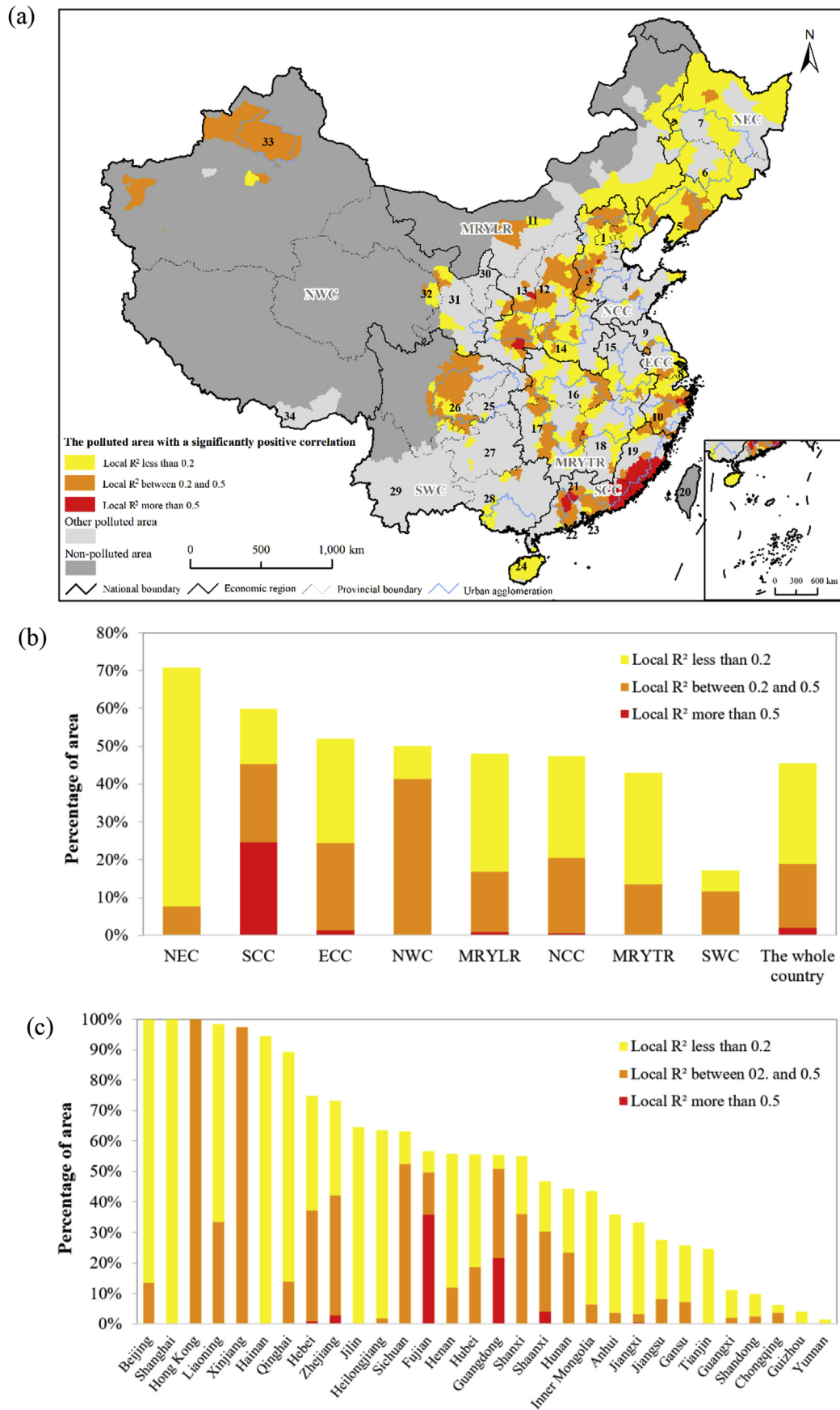


Fig. 5. The relationships between PM_{2.5} pollution and PLAND in China.

(a) The spatial patterns of the relationships. (b) The percentage of the total area of counties with significant positive relationships across each economic region. (c) The percentage of the total area of counties with significant positive relationships across each province.

Note: The names of the economic regions and provinces are listed in Fig. 1.

Table 4The relationships between the PM_{2.5} pollution and urban landscape patterns across the eight economic regions in China.

Regions	PLAND		PD		ED	
	Area (10 ⁴ km ²)	Percentage (%)	Area (10 ⁴ km ²)	Percentage (%)	Area (10 ⁴ km ²)	Percentage (%)
NEC	51.28	70.76	50.03	69.04	50.03	69.04
SCC	19.87	59.79	11.04	33.23	19.87	59.79
ECC	10.86	51.96	10.67	51.00	11.67	55.78
NWC	25.24	50.09	22.64	44.94	25.48	50.59
MRYL	48.16	48.02	46.57	46.42	49.54	49.39
NCC	17.51	47.48	17.44	47.28	17.78	48.20
MRYTR	30.31	42.98	28.48	40.38	30.67	43.48
SWC	17.30	17.16	19.73	19.58	21.13	20.97
The whole country	220.53	45.43	206.60	42.55	226.16	46.59

Note: Area: The total area of counties with a significant positive correlation.

Percentage: The total area of counties with a significant positive correlation as a percentage of the polluted area in the corresponding region.

randomness of the residuals (Anselin, 1995). Therefore, the GWR model effectively removed the influence attributable to the spatial autocorrelation of the variables when analyzing the relationships between the ULPs and PM_{2.5} pollution in China, indicating that the GWR model was more reliable than the other three models.

Our findings agree with the results of previous studies. For instance, Yu et al. (2013) found that the performance of the GWR model was significantly better than that of the OLS model in terms of quantifying the relationships between land use and water quality in Shenzhen. In addition, Li et al. (2017) found that the GWR model was more reliable than the OLS model when evaluating the impact of urbanization on the ULP in Beijing. Furthermore, Wang et al. (2014) analyzed the spatial variability of China's carbon footprint and found that the GWR model incorporated spatial elements into the regression, significantly improving the validity and effectiveness of the model.

5.2. There is a difference in the relationships between three urban landscape metrics and PM_{2.5} pollution

There were obvious spatial differences in the relationships between PLAND, PD, ED and PM_{2.5} pollution. At the national scale, the total areas with a significant correlation between the PLAND, PD, ED and PM_{2.5} pollution was 2.21×10^6 km², 2.07×10^6 km² and 2.26×10^6 km², respectively, accounting for 45.43%, 42.55% and 46.59%, respectively, of the entire polluted area in China (Fig. 8a). Among them, the total areas with strong relationships between PD/ED and PM_{2.5} pollution were 1.96×10^5 km² and 1.89×10^5 km², respectively, accounting for 4.04% and 3.89%, respectively, of the entire PM_{2.5}-polluted area. In contrast, the total area with a strong relationship between PLAND and PM_{2.5} pollution occupied less than 2% of the PM_{2.5}-polluted area. At the regional level, the effects of the PLAND and ED on PM_{2.5} pollution were mainly concentrated in SCC, while the relationships between the PD and PM_{2.5} pollution were closer in NWC. (Fig. 8b). The total areas characterized by a strong relationship between the PLAND/ED and PM_{2.5} pollution were 8.15×10^4 km² and 9.84×10^4 km², respectively, accounting for 24.53% and 29.60%, respectively, of the total PM_{2.5}-polluted area in SCC. In NWC, the area of PD closely related to PM_{2.5} pollution was 10.01×10^4 km², which accounted for 19.86% of the total polluted area. Focusing on the provinces in SCC and NWC, we found that the PLAND, PD and ED in Fujian Province all contributed significantly to PM_{2.5} pollution, and the area with local R² above 0.5 accounted for more than 20% of the total polluted area (Fig. 8c). There was a strong relationship between the PM_{2.5} pollution and the PLAND/ED in Guangdong Province, while there was a strong relationship between the PD and PM_{2.5} pollution in Xinjiang Province.

The causes of the differences may come from heating and traffic emissions. For NWC, the temperature in winter is extremely low,

and heating usually results in serious PM_{2.5} pollution (Huang et al., 2012; Li et al., 2018a). Compared to compact urban forms, urban landscape fragmentation with higher PD may lead to the lower efficiency of energy use (Liu et al., 2018a); for example, it is difficult to fully cover the central heating system. Traffic emissions represent the main contribution to PM_{2.5} pollution in SCC (Wu et al., 2013). Exhaust emissions from private cars are closely related to urban landscape shape (Zhou et al., 2018), and complex urban landscape shapes (i.e., higher ED) will have more chaos and traffic congestion, resulting in low-speed travel, longer driving times and more PM_{2.5} pollutants (Bereitschaft and Debbage, 2013). Simultaneously, affected by topography and climatic conditions, the transport of pollutants in Guangdong and Fujian may be exchanged with the free atmosphere across the mixing layer and limit the ability of the atmosphere to diffuse and transport pollutants (Li et al., 2018b). In addition, a higher PLAND value indicates less vegetation coverage and more impervious surfaces, which aggravates the urban heat island and further hinders the diffusion of atmospheric pollutants.

5.3. The ULPs in urban agglomerations (UAs) have a more significant impact on PM_{2.5} pollution

In the past 10 years, China has promoted UAs as the main areas in the implementation of the *National New-type Urbanization Plan (2014–2020)*, and thus, UAs have become the core zones in China's future urban development (Fang, 2015). With the rapid socioeconomic development in UAs, the urban landscape area continues to increase, and the PM_{2.5} pollution is becoming increasingly serious in these regions (Fang, 2015; He et al., 2017). Revealing the relationships between ULPs and PM_{2.5} pollution in UAs is of great significance for improving the sustainability of Chinese cities. Therefore, we further analyzed the relationships between the ULPs and PM_{2.5} pollution in 14 of China's major UAs, which were listed in the study by Fang (2015).

We found that the relationships between the ULPs and PM_{2.5} pollution in the UAs in China were obviously stronger than the relationship at the national level (Fig. 9a). The 14 major UAs were all located in PM_{2.5}-polluted regions, with a total polluted area of 1.40×10^6 km². The total area with a significant correlation between the ULPs and PM_{2.5} pollution (i.e., at least one ULP metric had a significant correlation with PM_{2.5} pollution) was 9.20×10^5 km², which accounted for 65.55% of the entire area of UAs in China. In addition, this total area was nearly 14% higher than the national average level. Eleven of the 14 UAs exhibited a significant correlation between the ULPs and PM_{2.5} pollution over more than half of the total agglomeration area. In particular, the entire area of the Northern Tianshan Mountains (NTM) UA exhibited a significant correlation between the ULPs and PM_{2.5} pollution therein. In four of

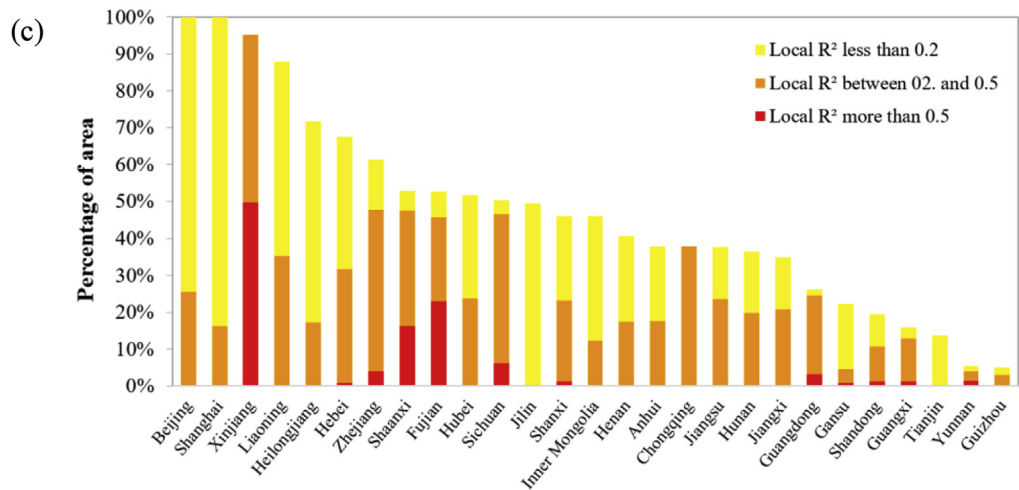
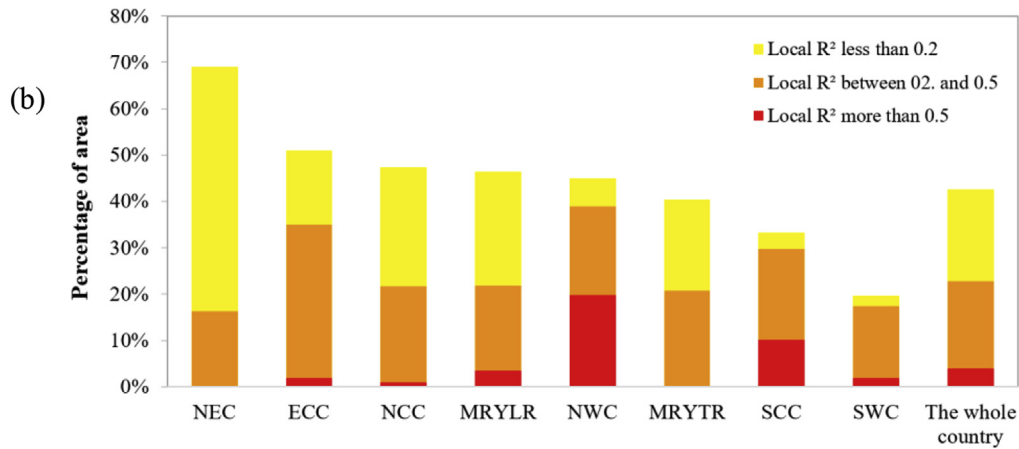
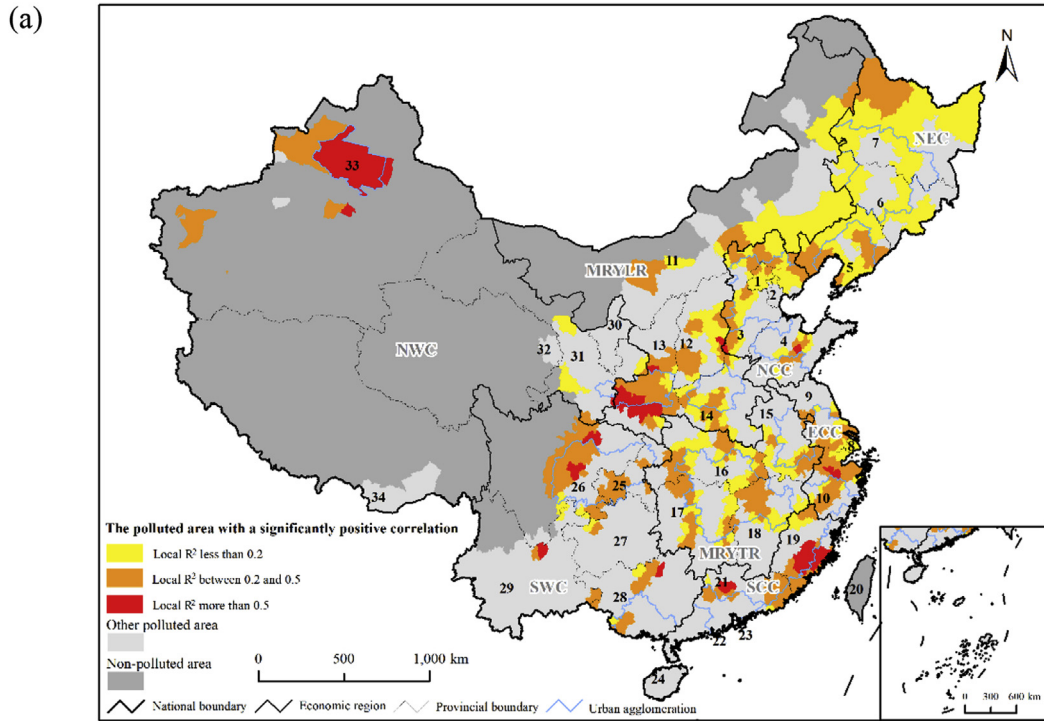


Fig. 6. The relationships between PM_{2.5} pollution and PD in China. (a) The spatial patterns of the relationships. (b) The percentage of the total area of counties with significant positive relationships across each economic region. (c) The percentage of the entire area of counties with significant positive relationships across each province. **Note:** The names of the economic regions and provinces are listed in Fig. 1.

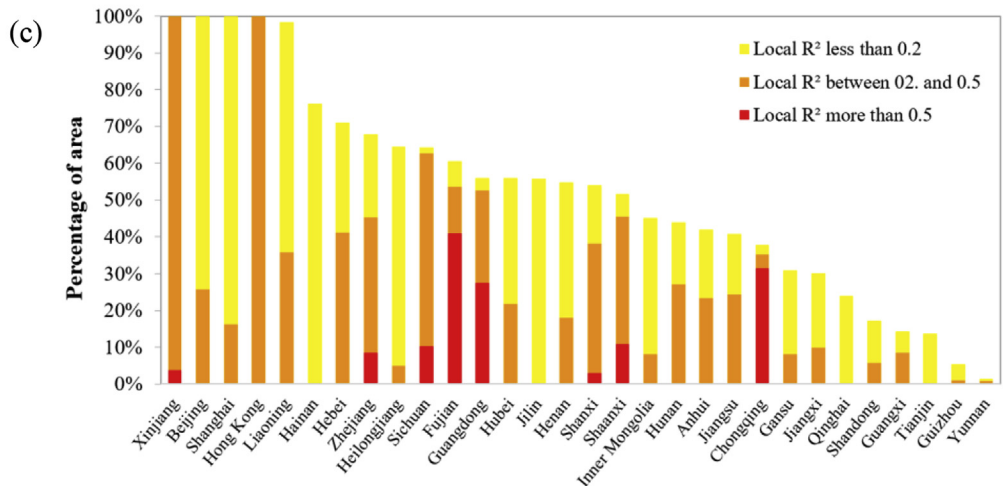
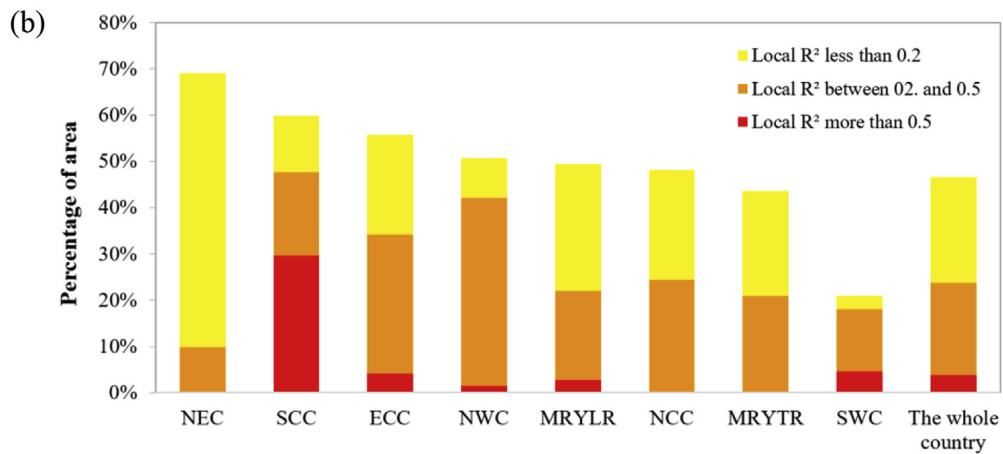
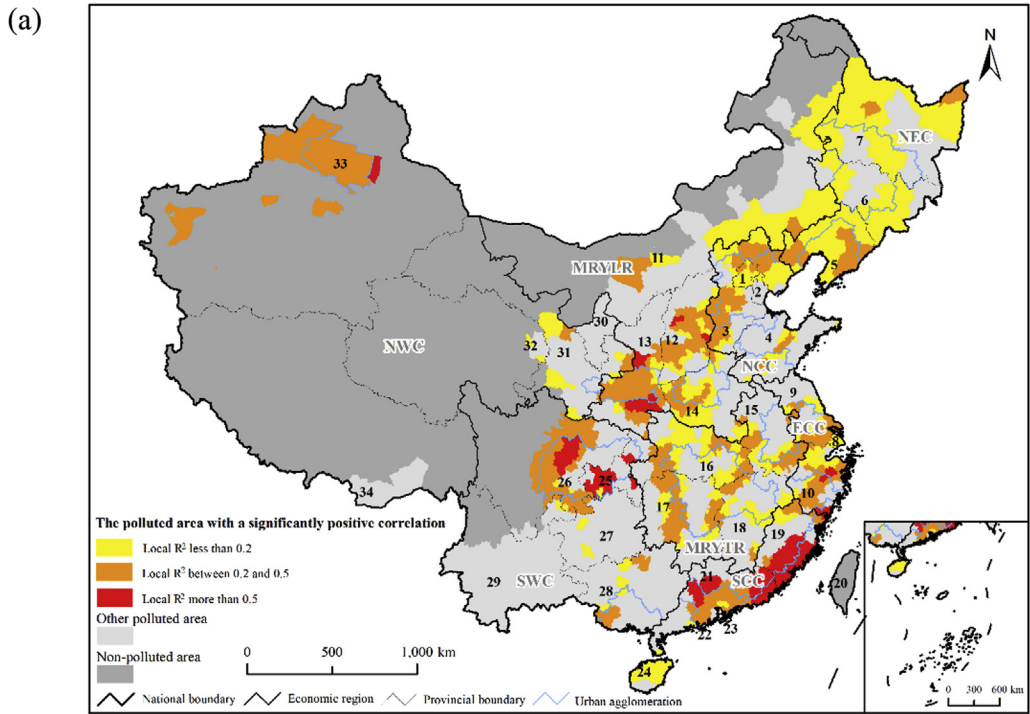


Fig. 7. The relationships between $PM_{2.5}$ pollution and ED in China.

(a) The spatial patterns of the relationships. (b) The percentage of the total area of counties with significant positive relationships across each economic region. (c) The percentage of the total area of counties with significant positive relationships across each province.

Note: The names of the economic regions and provinces are listed in Fig. 1.

Table 5

A comparison between the GWR model and the OLS/SLM/SEM model.

Indicators	PLAND	PD	ED
Adjusted R^2_{O}	0.045	0.064	0.062
Adjusted R^2_{SL}	0.893	0.893	0.894
Adjusted R^2_{SE}	0.897	0.897	0.898
Adjusted R^2_{G}	0.969	0.966	0.970
AIC _{CO}	-985.7	-1033.8	-1028.1
AIC _{CSL}	-5492.3	-5481.3	-5514.7
AIC _{CSE}	-5583.7	-5581.6	-5612.4
AIC _{CG}	-8525.5	-8357.5	-8595.5
I_{O}	0.771	0.745	0.763
I_{SL}	0.094	0.092	0.092
I_{SE}	0.084	0.083	0.083
I_{G}	0.089	0.063	0.084

Note: Adjusted R^2_{O} , Adjusted R^2_{SL} , Adjusted R^2_{SE} and Adjusted R^2_{G} denote the adjusted R^2 values of the OLS, SLM, SEM and GWR, respectively. AIC_{CO}, AIC_{CSL}, AIC_{CSE} and AIC_{CG} denote the AIC values of the OLS, SLM, SEM and GWR, respectively. I_{O} , I_{SL} , I_{SE} and I_{G} denote Moran's I calculated for the residuals from the OLS, SLM, SEM and GWR, respectively.

the UAs, namely, Central and Southern Liaoning (CSLN), Pearl River Delta (PRD), Guanzhong (GZH) and Western Taiwan Straits (WTS), the ratios of the areas where the PM_{2.5} pollution was positively correlated with the ULPs to the total areas of the corresponding UAs ranged from 80% to 100%. Among the other four UAs, namely, Beijing-Tianjin-Hebei (BTH), Yangtze River Delta (YRD), Central Plains (CPL) and Chengdu-Chongqing (CDCQ), the proportions of the areas with significant correlations between the ULPs and PM_{2.5} pollution among the total areas of the corresponding UAs ranged from 60% to 80%. In two of the UAs, namely, Harbin-Changchun (HBCC) and the Middle Yangtze (MYZ), the ratios of the areas with significant correlations between the ULPs and PM_{2.5} pollution to the total areas of the corresponding UAs ranged from 50% to 60%.

We also found that the PM_{2.5} pollution in UAs was jointly influenced by the area, the magnitude of fragmentation and the shape of the urban landscape (Fig. 9b). Among the 14 UAs, the total area characterized by significant relationships between the PM_{2.5} pollution and all three landscape metrics was $6.46 \times 10^5 \text{ km}^2$, occupying 70.23% of the entire area that had a significant correlation between the ULP and PM_{2.5} pollution. Twelve of the 14 UAs were characterized by PM_{2.5} pollution that was jointly influenced by the area, the magnitude of fragmentation and the shape of the landscape over more than half of the total agglomeration area. In particular, the entire NTM area displayed a significant correlation between PM_{2.5} pollution and all three landscape metrics. In CSLN, BTH and GZH, the ratios of the areas where the PM_{2.5} pollution was jointly influenced by all three landscape metrics to the total areas of the corresponding UAs ranged from 80% to 100%, while the ratios in eight other UAs, including YRD, WTS and HBCC, ranged from 50% to 80%.

Our findings agree with the results of previous studies. For instance, Liu et al. (2017a) found that the areas with the most serious PM_{2.5} pollution in China were concentrated mainly in UAs with a high population density; additionally, urban built-up areas had significant impacts on PM_{2.5} pollution. Furthermore, Du et al. (2018) found that the urbanization in the BTH and in the YRD and the PRD has had a significant impact on the PM_{2.5} pollution therein. Additionally, Wang and Fang (2016) indicated that PM_{2.5} pollution in the CSLN, BTH, and SDP was significantly associated with regional urbanization.

In 2014, the government of China began to implement the *National New-type Urbanization Plan (2014–2020)* for the sustainable development of cities. According to this plan, China's urbanization level will reach 60% by 2020 (Bai et al., 2014), and UAs will constitute the core areas of China's future urbanization. Therefore, in the process of promoting new-type urbanization plans, we

suggest that it is necessary to focus on the impacts of ULPs on PM_{2.5} pollution in UAs, especially in NTM, CSLN, PRD, GZH and WTS. In addition to strictly controlling the sprawl of urban land, it is necessary to improve the urban form and optimize the urban layout to reduce the impacts of ULPs on PM_{2.5} pollution.

5.4. Implications and future perspectives

In contrast with previous studies, our study fully considered the spatial autocorrelation and spatial differences between variables and improved the accuracy of measuring these relationships. We not only revealed the impacts of urban forms on PM_{2.5} pollution but also intuitively reflected the differences in the relationships between ULPs and PM_{2.5} pollution in different regions. Our study showed that the GWR method could effectively reveal the spatial relationships between ULPs and PM_{2.5} pollution in China. We also found that there was significant spatial heterogeneity in the relationships between ULPs and PM_{2.5} pollution in China. For example, the effects of the PLAND and ED on the PM_{2.5} pollution were mainly concentrated in SCC, while the relationship between the PD and the PM_{2.5} pollution was closer in NWC. Therefore, in the future, the government of China should focus on the effects of urban planning and construction on PM_{2.5} pollution. Both measures of controlling urban land sprawl and improving the urban form should be considered. For instance, the fragmentation of ULPs could be avoided by optimizing the urban spatial layout, rationally designing urban fringe, building a highly efficient urban road network system, and reducing the emission of atmospheric pollutants. In addition, the construction of urban interior space should be improved, and elements such as urban open spaces, atmospheric transport corridors and local diffusion conditions should be considered in a coordinated way to promote the *Prevention and Control of Atmospheric Pollution*.

This study does have some limitations. The spatial resolution of the urban land data was relatively low. Hence, when using these data, the urban patches with areas less than 1 km² cannot be identified, and thus, it is difficult to precisely analyze the ULP. Meanwhile, the PM_{2.5} data used in this study were obtained by satellite remote sensing technology, and although the data were calibrated according to the monitoring data in the data processing, the estimation of the PM_{2.5} concentration may still be lower than the actual observed value (Jerrett et al., 2017). Moreover, we analyzed only the statistical relationships between the ULPs and PM_{2.5} pollution based on the GWR model, without revealing the intrinsic mechanism causing the impacts of ULPs on PM_{2.5} pollution (Jayarathne et al., 2014; Li et al., 2016; Liang and Keener, 2015).

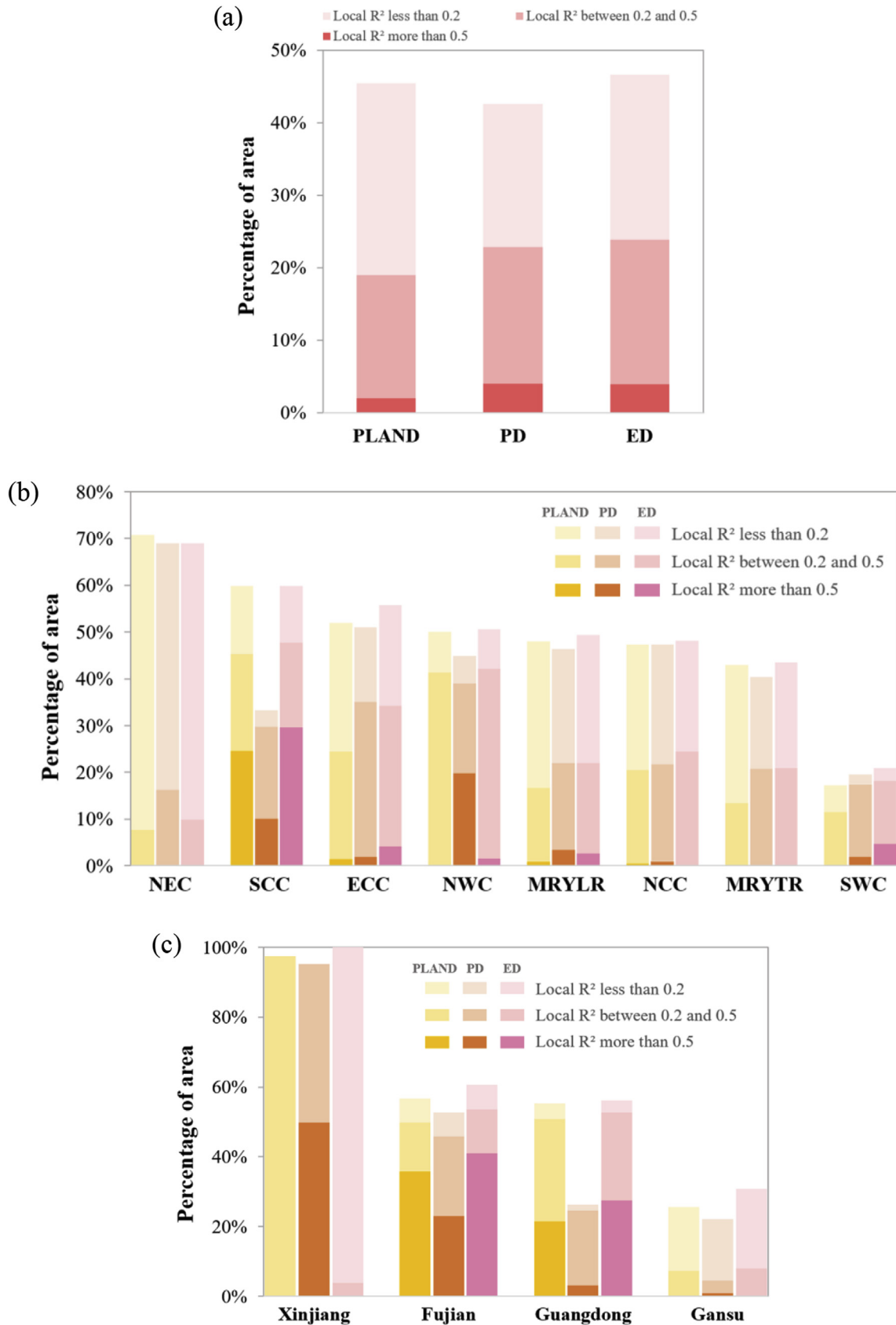


Fig. 8. Differences in the relationships between PM_{2.5} pollution and three urban landscape metrics.

(a) The percentage of the total area of counties with significant positive relationships at the national scale. (b) The differences in the relationships at the regional scale. (c) The differences in the relationships for the provinces in SCC and NWC.

Note: The names of the economic regions and provinces are listed in Fig. 1.

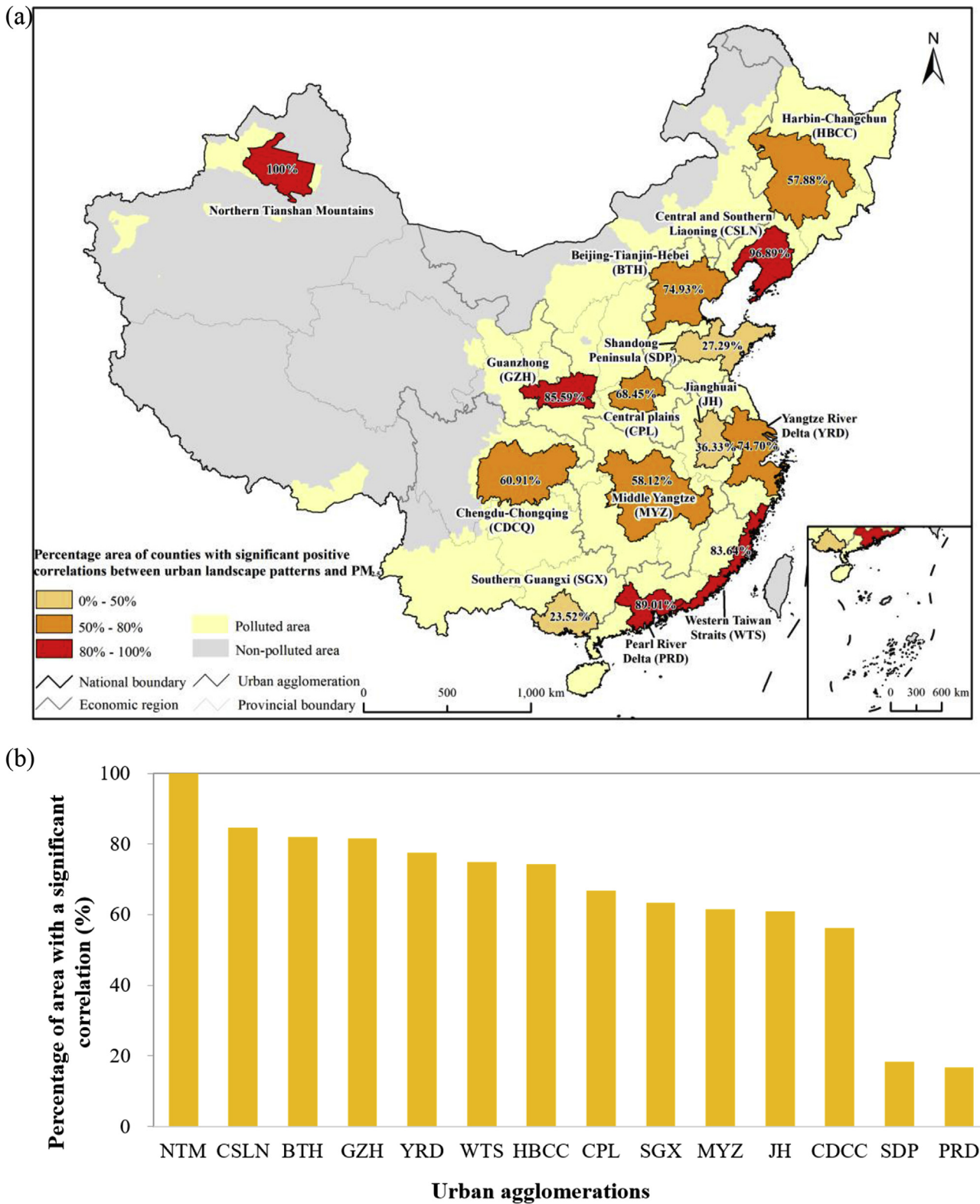


Fig. 9. The relationship between the PM_{2.5} pollution and urban landscape patterns across the major urban agglomerations (UAs). (a) The spatial patterns of the relationships between the PM_{2.5} pollution and urban landscape patterns in China. (b) The percentage of the area with a significant correlation between the PM_{2.5} pollution and urban landscape patterns in each UA.

In future studies, we will use new data with a finer spatial resolution to extract urban land (Zhang et al., 2013). At the same time, we will utilize a process-based model (e.g., the regional multiscale air quality model or positive matrix factorization) to reveal the internal mechanism driving the impacts of ULPs on PM_{2.5} pollution (Hou et al., 2015; Liu et al., 2017b).

6. Conclusions

The relationships between ULPs and PM_{2.5} pollution exhibited obvious spatial heterogeneity. The areas with significant relationships for ED-PM_{2.5}, PLAND-PM_{2.5} and PD-PM_{2.5} were 2.26×10^6 km², 2.21×10^6 km² and 2.07×10^6 km², respectively, occupying 46.59%, 45.43% and 42.55%, respectively, of the total area of PM_{2.5} polluted regions in China. The relationships for ED-PM_{2.5} and PLAND-PM_{2.5} were the strongest in Fujian and Guangdong, while the relationship between the PD and PM_{2.5} pollution was the strongest in Xinjiang.

The relationships between the ULPs and PM_{2.5} pollution in UAs were obviously stronger than the relationships at the national level. The area with a significant correlation between the ULPs and PM_{2.5} pollution was 9.20×10^5 km², occupying 65.55% of the entire area of UAs; in addition, this proportion was nearly 14% higher than the national level. The relationship between the ULPs and PM_{2.5} pollution was the strongest in the NTM.

This study fully considered the spatial autocorrelation and spatial differences between variables using the GWR model, clarified the spatial heterogeneity of the relationships between ULPs and PM_{2.5} pollution, and provided reliable information for supporting sustainable urban landscape planning in China. We consequently suggest that the Chinese Government should consider the spatial characteristics of the relationships between ULPs and PM_{2.5} pollution in different regions and focus on the ULPs in the UAs, particularly those in five UAs, including the NTM, the CSLN and the PRD, during the promotion of new-type urbanization plans. Controlling urban land sprawl and improving the urban form should help reduce the impacts of ULPs on PM_{2.5} pollution and improve urban sustainability in China.

Acknowledgements

We want to express our respect and gratitude to the anonymous reviewers and editors for their professional comments and suggestions. This work was supported in part by the National Natural Science Foundation of China (grant no. 41621061 & 41871185). It was also supported by the Fundamental Research Funds for the Central Universities and the project from State Key Laboratory of Earth Surface Processes and Resource Ecology, China.

References

- Anselin, L., 1988. Spatial econometrics: methods and models. In: *Spatial Econometrics: Methods and Models*. Springer Netherlands.
- Anselin, L., 1995. Local indicators of spatial association—LISA. *Geogr. Anal.* 27 (2), 93–115. <https://doi.org/10.1111/j.1538-4632.1995.tb00338.x>.
- Bai, X., Shi, P., Liu, Y., 2014. Realizing China's urban dream. *Nature* 509 (7499), 158–160. <https://doi.org/10.1038/509158a>.
- Battaglia, M.A., Douglas, S., Hennigan, C.J., 2017. Effect of the urban heat island on aerosol PH. *Environ. Sci. Technol.* 51 (22), 13095–13103. <https://doi.org/10.1021/acs.est.7b02786>.
- Bereitschaft, B., Debbage, K., 2013. Urban form, air pollution, and CO₂ emissions in large US metropolitan areas. *Prof. Geogr.* 65 (4), 612–635. <https://doi.org/10.1080/00330124.2013.799991>.
- Borrego, C., Martins, H., Tchepel, O., Salmim, L., Monteiro, A., Miranda, A.I., 2006. How urban structure can affect city sustainability from an air quality perspective. *Environ. Model. Softw.* 21 (4), 461–467. <https://doi.org/10.1016/j.envsoft.2004.07.009>.
- Brunsdon, C., Fotheringham, A.S., Charlton, M.E., 1996. Geographically weighted regression: a method for exploring spatial non-stationarity. *Geogr. Anal.* 28 (4), 281–298. <https://doi.org/10.1111/j.1538-4632.1996.tb00936.x>.
- Brunsdon, C., Fotheringham, A.S., Charlton, M.E., 1998. Spatial nonstationarity and autoregressive models. *Environ. Plan.* 30 (6), 957–973. <https://doi.org/10.1068/a300957>.
- Clement, F., Orange, D., Williams, M., Mulley, C., Epprecht, M., 2009. Drivers of afforestation in northern Vietnam: assessing local variations using geographically weighted regression. *Appl. Geogr.* 29 (4), 561–576. <https://doi.org/10.1016/j.apgeog.2009.01.003>.
- Du, Y., Sun, T., Peng, J., Fang, K., Liu, Y., Yang, Y., 2018. Direct and spillover effects of urbanization on PM_{2.5} concentrations in China's top three urban agglomerations. *J. Clean. Prod.* 190, 72–83. <https://doi.org/10.1016/j.jclepro.2018.03.290>.
- Fang, C., 2015. Important progress and future direction of studies on China's urban agglomerations. *J. Geogr. Sci.* 25 (8), 1003–1024. <https://doi.org/10.1007/s11442-015-1216-5>.
- Forman, R.T.T., 2014. *Urban Ecology: Science of Cities*. Cambridge University Press, New York.
- Fotheringham, A.S., Brunsdon, C., Charlton, M.E., 2002. *Geographically Weighted Regression: the Analysis of Spatially Varying Relationships*. Wiley, New York.
- Han, L., Zhou, W., Li, W., 2015. Increasing impact of urban fine particles (PM_{2.5}) on areas surrounding Chinese cities. *Sci. Rep.* 5, 12567. <https://doi.org/10.1038/srep12467>.
- Han, L., Zhou, W., Li, W., Li, L., 2014. Impact of urbanization level on urban air quality: a case of fine particles (PM_{2.5}) in Chinese cities. *Environ. Pollut.* 194C (1), 163. <https://doi.org/10.1016/j.envpol.2014.07.022>.
- He, C., Gao, B., Huang, Q., Ma, Q., Dou, Y., 2017. Environmental degradation in the urban areas of China: evidence from multi-source remote sensing data. *Remote Sens. Environ.* 193, 65–75. <https://doi.org/10.1016/j.rse.2017.02.027>.
- He, C., Han, L., Zhang, R., 2016. More than 500 million Chinese urban residents (14% of the global urban population) are imperiled by fine particulate hazard. *Environ. Pollut.* 218, 558–562. <https://doi.org/10.1016/j.envpol.2016.07.038>.
- He, C., Liu, Z., Tian, J., Ma, Q., 2014. Urban expansion dynamics and natural habitat loss in China: a multiscale landscape perspective. *Glob. Chang. Biol.* 20 (9), 2886–2902. <https://doi.org/10.1111/gcb.12553>.
- Hou, X., Strickland, M.J., Liao, K., 2015. Contributions of regional air pollutant emissions to ozone and fine particulate matter-related mortalities in eastern US urban areas. *Environ. Res.* 137, 475–484. <https://doi.org/10.1016/j.envres.2014.10.038>.
- Huang, B., Yang, H., Mauerhofer, V., Guo, R., 2012. Sustainability assessment of low carbon technologies—case study of the building sector in China. *J. Clean. Prod.* 32, 244–250. <https://doi.org/10.1016/j.jclepro.2012.03.031>.
- Huang, R., Zhang, Y., Bozzetti, C., Ho, K., Cao, J., Han, Y., Daellenbach, K.R., Slowik, J.G., Platt, S.M., Canonaco, F., Zotter, P., Wolf, R., Pieber, S.M., Bruns, E.A., Crippa, M., Ciarelli, G., Piazzalunga, A., Schwikowski, M., Abbaszade, G., Schnelle-Kreis, J., Zimmermann, R., An, Z., Szidat, S., Baltensperger, U., El Haddad, I., Prevot, A.S.H., 2014. High secondary aerosol contribution to particulate pollution during haze events in China. *Nature* 514 (7521), 218–222. <https://doi.org/10.1038/nature13774>.
- Irwin, E.G., Bockstael, N.E., 2007. The evolution of urban sprawl: evidence of spatial heterogeneity and increasing land fragmentation. *Prac. Natl. Acad. Sci.* 104 (52), 20672–20677. <https://doi.org/10.1073/pnas.0705527105>.
- ISO, 1994. ISO 4225: Air Quality-General Aspects—Vocabulary. Retrieved from: https://www.iso.org/standard/10025.html?tdsourcetag=s_pctim_aiomsg.
- Jayarathne, T., Stockwell, C.E., Yokelson, R.J., Nakao, S., Stone, E.A., 2014. Emissions of fine particle fluoride from biomass burning. *Environ. Sci. Technol.* 48 (21), 12636–12644. <https://doi.org/10.1021/es502933>.
- Jerrett, M., Turner, M.C., Beckerman, B.S., 2017. Comparing the health effects of ambient particulate matter estimated using ground-based versus remote sensing exposure estimates. *Environ. Health Perspect.* 125 (4), 552–559. <https://doi.org/10.1289/EHP575>.
- Jiang, P., Yang, J., Huang, C., Liu, H., 2017. The contribution of socioeconomic factors to PM_{2.5} pollution in urban China. *Environ. Pollut.* 233, 977–985. <https://doi.org/10.1016/j.envpol.2017.09.090>.
- Larkin, A., van Donkelaar, A., Geddes, J.A., Martin, R.V., Hyatt, P., 2016. Relationships between changes in urban characteristics and air quality in East Asia from 2000 to 2010. *Environ. Sci. Technol.* 50 (17), 9142–9149. <https://doi.org/10.1021/acs.est.6b02549>.
- Li, G., Fang, C., Wang, S., Sun, S., 2016. The effect of economic growth, urbanization, and industrialization on fine particulate matter (PM_{2.5}) concentrations in China. *Environ. Sci. Technol.* 50 (21), 11452. <https://doi.org/10.1021/acs.est.6b02562>.
- Li, H., Peng, J., Liu, Y., Hu, Y., 2017. Urbanization impact on landscape patterns in Beijing city, China: a spatial heterogeneity perspective. *Ecol. Indic.* 82, 50–60. <https://doi.org/10.1016/j.ecolind.2017.06.032>.
- Li, H., You, S., Zhang, H., Zheng, W., Lee, W., Ye, T., Zou, L., 2018a. Analyzing the impact of heating emissions on air quality index based on principal component regression. *J. Clean. Prod.* 171, 1577–1592. <https://doi.org/10.1016/j.jclepro.2017.10.106>.
- Li, T., Deng, X., Li, Y., Song, Y., Li, L., Tan, H., Wang, C., 2018b. Transport paths and vertical exchange characteristics of haze pollution in Southern China. *Sci. Total Environ.* 625, 1074–1087. <https://doi.org/10.1016/j.scitotenv.2017.12.235>.
- Liang, M., Keener, T., 2015. Atmospheric feedback of urban boundary layer with implications for climate adaptation. *Environ. Sci. Technol.* 49 (17), 10598–10606. <https://doi.org/10.1021/acs.est.5b02444>.
- Liu, H., Fang, C., Zhang, X., Wang, Z., Bao, C., Li, F., 2017a. The effect of natural and anthropogenic factors on haze pollution in Chinese cities: a spatial econometrics approach. *J. Clean. Prod.* 165, 323–333.

- [jjclepro.2017.07.127](#).
- Liu, B., Wu, J., Zhang, J., Wang, L., Yang, J., Liang, D., Dai, Q., Bi, X., Feng, Y., Zhang, Y., Zhang, Q., 2017b. Characterization and source apportionment of PM_{2.5} based on error estimation from EPA PMF 5.0 model at a medium city in China. *Environ. Pollut.* 222, 10–22. <https://doi.org/10.1016/j.envpol.2017.01.005>.
- Liu, Y., Wu, J., Yu, D., 2018a. Disentangling the complex effects of socioeconomic, climatic, and urban form factors on air pollution: a case study of China. *Sustainability* 10 (3), 776. <https://doi.org/10.3390/su10030776>.
- Liu, Y., Wu, J., Yu, D., Ma, Q., 2018b. The relationship between urban form and air pollution depends on seasonality and city size. *Environ. Sci. Pollut. Res.* 25 (16), 1–14. <https://doi.org/10.1007/s11356-018-1743-6>.
- Liu, Z., He, C., Zhou, Y., Wu, J., 2014. How much of the world's land has been urbanized, really? A hierarchical framework for avoiding confusion. *Landscape Ecol.* 29 (5), 763–771. <https://doi.org/10.1007/s10980-014-0034-y>.
- Liu, Z., Ding, M., He, C., Li, J., Wu, J., 2019. The impairment of environmental sustainability due to rapid urbanization in the dryland region of northern China. *Landscape Urban Plan.* 187, 165–180. <https://doi.org/10.1016/j.landurbplan.2018.10.020>.
- Lu, D., Mao, W., Yang, D., Zhao, J., Xu, J., 2018. Effects of land use and landscape pattern on PM_{2.5} in Yangtze River Delta, China. *Atmos. Pollut. Res.* 9 (4), 705–713. <https://doi.org/10.1016/j.apr.2018.01.012>.
- Su, S., Xiao, R., Zhang, Y., 2012. Multi-scale analysis of spatially varying relationships between agricultural landscape patterns and urbanization using geographically weighted regression. *Appl. Geogr.* 32 (2), 360–375. <https://doi.org/10.1016/j.apgeog.2011.06.005>.
- Tu, J., 2011. Spatially varying relationships between land use and water quality across an urbanization gradient explored by geographically weighted regression. *Appl. Geogr.* 31 (1), 376–392. <https://doi.org/10.1016/j.apgeog.2010.08.001>.
- van Donkelaar, A., Martin, R.V., Brauer, M., Hsu, N.C., Kahn, R.A., Levy, R.C., Lyapustin, A., Sayer, A.M., Winker, D.M., 2016. Global estimates of fine particulate matter using a combined geophysical-statistical method with information from satellites, models, and monitors. *Environ. Sci. Technol.* 50 (7), 3762–3772. <https://doi.org/10.1021/acs.est.5b05833>.
- Wang, L., Wang, S., Zhou, Y., Liu, W., Hou, Y., Zhu, J., Wang, F., 2018. Mapping population density in China between 1990 and 2010 using remote sensing. *Remote Sens. Environ.* 210, 269–281. <https://doi.org/10.1016/j.rse.2018.03.007>.
- Wang, S., Fang, C., Ma, H., Wang, Y., Qin, J., 2014. Spatial differences and multi-mechanism of carbon footprint based on GWR model in provincial China. *J. Geogr. Sci.* 24 (4), 612–630. <https://doi.org/10.1007/s11442-014-1109-z>.
- Wang, Z., Fang, C., 2016. Spatial-temporal characteristics and determinants of PM_{2.5} in the Bohai rim urban agglomeration. *Chemosphere* 148 (148), 148–162. <https://doi.org/10.1016/j.chemosphere.2015.12.118>.
- WHO, 2005. WHO Air Quality Guidelines for Particulate Matter, Ozone, Nitrogen Dioxide and Sulfur Dioxide. Retrieved from: http://apps.who.int/iris/bitstream/10665/69477/1/WHO_SDE_PHE_OEH_06.02_eng.pdf.
- Wu, J., Jenerette, G.D., Buyantuyev, A., Redman, C.L., 2011. Quantifying spatiotemporal patterns of urbanization: the case of the two fastest growing metropolitan regions in the United States. *Ecol. Complex.* 8 (1), 0–8. <https://doi.org/10.1016/j.ecocom.2010.03.002>.
- Wu, D., Fung, J., Yao, T., Lau, A.K.H., 2013. A study of control policy in the Pearl River Delta region by using the particulate matter source apportionment method. *Atmos. Environ.* 76, 147–161. <https://doi.org/10.1016/j.atmosenv.2012.11.069>. Sp. Iss. SI.
- Wu, J., Xie, W., Li, W., Li, J., 2015. Effects of urban landscape pattern on PM_{2.5} pollution—a Beijing case study. *PLoS One* 10 (11), e0142449. <https://doi.org/10.1371/journal.pone.0142449>.
- Xu, H., Cao, J., Chow, J., Huang, R., Shen, Z., Chen, L., Ho, K., Watson, J.G., 2016a. Inter-annual variability of wintertime PM_{2.5} chemical composition in Xi'an, China: evidences of changing source emissions. *Sci. Total Environ.* 545, 546–555. <https://doi.org/10.1016/j.scitotenv.2015.12.070>.
- Xu, M., He, C., Liu, Z., Dou, Y., 2016b. How did urban land expand in China between 1992 and 2015? A multi-scale landscape analysis. *PLoS One* 11 (5), e0154839. <https://doi.org/10.1371/journal.pone.0154839>.
- Yang, X., Wang, S., Zhang, W., Zhan, D., Li, J., 2017. The impact of anthropogenic emissions and meteorological conditions on the spatial variation of ambient SO₂ concentrations: a panel study of 113 Chinese cities. *Sci. Total Environ.* 584, 318–328. <https://doi.org/10.1016/j.scitotenv.2016.12.145>.
- Yu, D., 2006. Spatially varying development mechanisms in the greater Beijing area: a geographically weighted regression investigation. *Ann. Reg. Sci.* 40 (1), 173–190. <https://doi.org/10.1007/s00168-005-0038-2>.
- Yu, D., Shi, P., Liu, Y., Xun, B., 2013. Detecting land use-water quality relationships from the viewpoint of ecological restoration in an urban area. *Ecol. Eng.* 53 (3), 205–216.
- Yuan, M., Huang, Y., Shen, H., Li, T., 2018. Effects of urban form on haze pollution in China: spatial regression analysis based on PM_{2.5} remote sensing data. *Appl. Geogr.* 98, 215–223. <https://doi.org/10.1016/j.ecoleng.2012.12.045>.
- Zhang, F., Chen, X., Vitousek, P., 2013. Chinese agriculture: an experiment for the world. *Nature* 497 (7447), 33–35. <https://doi.org/10.1038/497033a>.
- Zhang, X., Gong, Z., 2018. Spatiotemporal characteristics of urban air quality in China and geographic detection of their determinants. *J. Geogr. Sci.* 28 (5), 563–578. <https://doi.org/10.1007/s11442-018-1491-z>.
- Zhou, C., Li, S., Wang, S., 2018. Examining the impacts of urban form on air pollution in developing countries: a case study of China's megacities. *Int. J. Environ. Res. Public Health* 15 (8). <https://doi.org/10.3390/ijerph15081565>.